Measurement of the Carbon Isotopic Composition of Methane Using Helicoidal Laser Eigenstates

D. Jacob, A. Le Floch, F. Bretenaker, P. Guenot

Measurement of the Carbon Isotopic Composition of Methane Using Helicoidal Laser Eigenstates

D. Jacob ([1]), A. Le Floch ([1]), F. Bretenaker ([1,*]) and P. Guenot ([2])

([1]) Laboratoire d'Electronique Quantique - Physique des Lasers (**), Université de Rennes I, Campus de Beaulieu, F-35042 Rennes Cedex, France
([2]) Centre Régional de Mesures Physiques de l'Ouest, Université de Rennes I, Campus de Beaulieu, F-35042 Rennes Cedex, France

(Received 13 December 1995, received in final form 28 February 1996, accepted 5 March 1996)

PACS.42.60.By - Design of specific laser systems
PACS.07.07.Df - Sensors (chemical, optical, electrical, movement, gas, etc.); remote sensing

Abstract. — The spatially generalized Jones matrix formalism is used to design a laser cavity to make intracavity measurements of the carbon isotopic composition of methane. The method is based on a double optical lever effect for helicoidally polarized eigenstates, permitting to measure successively the $^{12}CH_4$ and $^{13}CH_4$ concentrations. To choose the probed isotope, one simply tunes the frequency of the laser by Zeeman effect. The experiment exhibits a good agreement with the predictions and permits to measure the $^{13}CH_4/^{12}CH4$ composition ratio of methane with an uncertainty of the order of $\pm 0.07\%$ for a sample containing only 6×10^{-9} mole of methane.

Résumé. — On utilise le formalisme des matrices de Jones généralisées spatialement pour concevoir une cavité laser permettant la mesure intra-cavité de la composition isotopique du carbone présent dans le méthane. La méthode est fondée sur une double application de l'effet de levier optique pour les états propres hélicoïdaux, permettant de mesurer successivement les concentrations de $^{12}CH_4$ et de $^{13}CH_4$. Pour passer d'un isotope à l'autre, on ajuste simplement la fréquence du laser par effet Zeeman. L'expérience est en bon accord avec les prédictions et permet d'effectuer la mesure du rapport isotopique $^{13}CH_4/^{12}CH_4$ avec une fourchette d'incertitude de $\pm 0,07$ % pour des échantillons de gaz ne contenant que 6×10^{-9} mole de méthane.

1. Introduction

Although methane is present only as a trace gas in the atmosphere, it plays an important role in the greenhouse effect and in the evolution of the climate. Indeed, researches on the evolution of the climate, both past [1] and present [2], show that a strong correlation exists between the concentration of methane in the atmosphere and the climate temperature. In order to establish a global atmospheric CH_4 budget, one has to realize isotopic composition measurements. Indeed, the different CH_4 sources have characteristic isotopic compositions, in particular concerning

(*) Author for correspondence (fax: 99 28 67 50, Rennes)
(**) Unité Associée Centre National de la Recherche Scientifique 1202

their $^{13}CH_4/^{12}CH_4$ production ratios. For atmospheric methane, the ratio $^{13}CH_4/^{12}CH_4$ is typically of the order of 1.1%. However, depending on the nature of the methane source, the changes of this isotopic ratio can typically vary from a few 0.001% to 0.1% [3,4]. In order to measure such small variations of isotopic ratios, one usually uses gas chromatographs coupled to mass spectrometers. This destructive method permits to reach precisions of the order of a few 10^{-6} for the ratio $^{13}CH_4/^{12}CH_4$. However, recently, non destructive optical absorption methods have been proposed to measure the $^{13}CH_4/^{12}CH_4$ isotopic ratio of methane [5,6]. One of these experiments [6] is based on the measurement of the absorption of the light emitted by a tunable diode laser in the 3.3 μm wavelength range propagating through a multipass cell. This method permits to reach a precision of 5×10^{-6} for the measurement of $^{13}CH_4/^{12}CH_4$ for 2 μmol of methane for a 213 m-long optical path through the multipass cell (71 roundtrips through a 1.5 m-long cell). Besides, it has recently been shown that intracavity absorption measurements using a two-eigenstate laser in a quasi-critical regime could lead to the existence of an optical lever effect for very sensitive measurements of $^{12}CH_4$ concentration [7]. Indeed, hard competition between laser eigenstates and spatial separation of these eigenstates has been shown to permit the detection of 5×10^{-15} mole of $^{12}CH_4$ for a 20 cm-long optical path. The aim of this paper is consequently to show how this optical lever method can be applied to the *non-destructive* measurement of the $^{13}CH_4/^{12}CH_4$ *isotopic ratio* of methane for a relatively short optical path and a *small quantity of gas*. In Section 2, after having recalled the principle of the optical lever effect, we predict from the spatially generalized Jones matrix formalism [8] how this principle can be applied to helicoidal laser eigenstates in order to measure the methane isotopic ratio. Section 3 is then devoted to the experimental verification of these predictions, to the double measurement of the isotopic composition of sample methane, and to the determination of the precision of the method. Finally, Section 4 discusses these results.

2. Theoretical Predictions

As stated in the Introduction, before discussing the new method based on helicoidal eigenstates that we used to measure the isotopic composition of methane, we first recall the principle of the optical lever method we applied to linearly polarized eigenstates to measure small quantities of $^{12}CH_4$ using a optical lever $^3He - ^{22}Ne$ laser oscillating at 3.39 μm [7].

2.1. Background: Optical Lever Effect for Linearly Polarized Eigenstates. — Let us consider a longitudinally and transversally monomode laser sustaining the oscillation of two eigenstates, as schematized in Figure 1. These eigenstates are spatially separated in one part of the cavity thanks to the introduction inside the cavity of a birefringent crystal creating a polarization walk-off. The eigenstates are then an ordinary and an extraordinary perpendicularly linearly polarized eigenstates of intensities I_0 and I_e [8]. Their eigenfrequencies are tuned so that their frequency difference is equal to a half-intermode range. Indeed, this choice permits to eliminate some systematic errors, as will be seen later. The active medium is introduced in the part of the cavity where the propagation axes of the two eigenstates are degenerate, in order to introduce some coupling between the eigenstates. The amount of coupling is parameterized by the coupling constant C [9]. For $C > 1$, the two eigenstates cannot oscillate simultaneously: they exhibit vectorial bistability. On the contrary, for $C < 1$, the two eigenstates can oscillate simultaneously for some ranges of the cavity frequency tuning. In this case, the two eigenstates share the energy available from the laser. If the two eigenstates have the same gain and losses and are tuned symmetrically with respect to the gain curve central

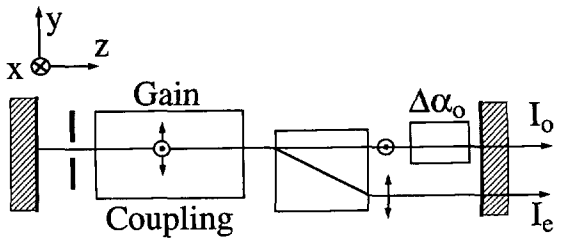

Fig. 1. — Optical lever laser with linearly polarized eigenstates. The two eigenstates are coupled thanks to the active medium. The observation of the output intensities I_0 and I_e of the two eigenstates leads to a levered measurement of the losses $\Delta\alpha_0$ created by the probed gas.

frequency, their intensities are equal and are given by:

$$I_0 = I_e \equiv I = \frac{1}{1+\sqrt{C}}\frac{\alpha}{\beta}, \tag{1}$$

where α and β are the common net gain and self-saturation coefficients of the two eigenstates [9]. Then, starting from this perfectly symmetrical situation, one introduces the sample to be measured on the path of one of the eigenstates, for example the ordinary eigenstates. This is performed by introducing the gas to be analyzed in a cell located on the path of the ordinary eigenstate only, in the part of the cavity where the two eigenstates are spatially separated. The sample gas contains $^{12}CH_4$ which creates losses, *i.e.*, which introduces a variation $\Delta\alpha_0$ of the net gain of the ordinary eigenstates. This has been shown [7] to lead to the following relative variations in intensity in the two eigenstates:

$$\frac{\Delta I_0}{I} = \frac{1}{1-\sqrt{C}}\frac{\Delta\alpha_0}{\alpha}, \tag{2a}$$

$$\frac{\Delta I_e}{I} = -\frac{\sqrt{C}}{1-\sqrt{C}}\frac{\Delta\alpha_0}{\alpha} \tag{2b}$$

In particular, in the case where $C \lesssim 1$ (quasi-critical coupling), equations (2) lead to:

$$\frac{\Delta I_0}{I} \approx -\frac{\Delta I_e}{I} = \frac{1}{1-\sqrt{C}}\frac{\Delta\alpha_0}{\alpha} \tag{3}$$

Equation (3) shows that the changes in intensity in the two eigenstates are complementary and vary linearly with $\Delta\alpha_0$. Moreover, the multiplicative factor $1/(1-\sqrt{C})$ shows that the sensitivity of the system is levered by the quasi-critical coupling ($C \lesssim 1$) regime. One can then define an optical lever arm factor OL as the gain of sensitivity obtained here over that of an extracavity measurement. From equation (3), this factor is given by:

$$OL = \frac{1}{1-\sqrt{C}}\frac{c}{2d}\frac{1}{\alpha}, \tag{4}$$

where c is the velocity of light and d the length of the laser cavity.

In reference [7], optical lever factors OL as high as 500 have been obtained for the detection of $^{12}CH_4$ in a $^3He - ^{22}Ne$ laser oscillating at 3.39 μm. This has permitted to reach a detection sensitivity of 3×10^9 molecules of $^{12}CH_4$ in vacuum, corresponding to 0.6 ppb m (part per billion times meter) in one atmosphere of air. In the following subsection, we predict how this optical lever method can be implemented to measure the carbon isotopic ratio $^{13}CH_4/^{12}CH_4$ of methane.

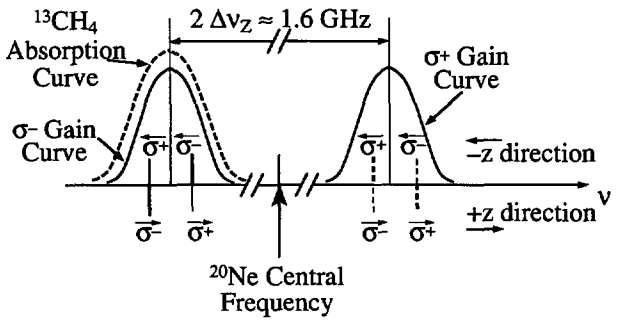

Fig. 2. — Full lines: σ^+ and σ^- gain profiles of ^{20}Ne shifted by a longitudinal magnetic field. The $^{13}CH_4$ absorption profile (dashed line) is in coincidence with the σ^- gain profile of ^{20}Ne. Notice the two groups of two helicoidally polarized eigenstates of the optical lever laser, corresponding to two different longitudinal modes of the laser. The one in dashed lines must be turned off, leaving only the eigenstates which coincide with the $^{13}CH_4$ absorption profile. Those latter eigenstates are amplified only in the direction of propagation for which they have a σ^- polarization.

2.2. Optical Lever Effect for Helicoidally Polarized Zeeman-Shifted Eigenstates. — The absorption lines of $^{13}CH_4$ are shifted by 300 GHz relatively to the absorption lines of $^{12}CH_4$ [10]. Fortunately, there exists an absorption line of $^{13}CH_4$ [$P(6)F_2^{(2)}$ component of the ν_3 band] which is only down-shifted of 810 MHz with respect to the $3s_2 \rightarrow 3p_4$ laser line of ^{20}Ne at 3.3922 μm. This line has an absorption coefficient equal to 0.2 $Torr^{-1}$ cm^{-1}, which is of the same order of magnitude of the absorption coefficient (0.17 $Torr^{-1}$ cm^{-1}) of the usual $^{12}CH_4$ absorption line [$P(7)F_2^{(2)}$ component of the ν_3 band] used in reference [7]. At low pressure, the Doppler widths of the $^{13}CH_4$ and $^{12}CH_4$ absorption lines are of the order of 300 MHz. Consequently, these two lines do not overlap and can be selectively probed thanks to a laser. The situation for $^{13}CH_4$ is summarized in Figure 2: the absorption line is down-shifted with respect to the ^{20}Ne emission line. To make the gain curve coincide with the selected absorption line, we use a longitudinal magnetic field of magnitude B. This field splits the ^{20}Ne gain curves into a σ^+ and a σ^- gain curves separated by a frequency difference $2\Delta\nu_Z$ with $\Delta\nu_Z/B \approx 1.58$ MHz G^{-1}. Then, for $B \approx 510$ G, one obtains the situation sketched in Figure 2: the σ^- gain curve coincides with the $^{13}CH_4$ absorption curve. However, there also exists a σ^+ gain curve at approximately 1.6 GHz of the σ^- gain curve.

To realize the optical lever experiment for $^{13}CH_4$, we must consequently build a laser which realizes the following conditions with $B \approx 510$ G: i) the laser must sustain oscillation of two quasi-critically coupled eigenstates with eigenfrequencies located in the σ^- gain curve and separated by $c/4d$; ii) the laser eigenstates (corresponding to another longitudinal mode) which could oscillate thanks to the σ^+ gain curve must be turned off. Moreover, for $B \approx 0$, the system must be able to measure the $^{12}CH_4$ concentration. To realize these conditions, we propose the laser cavity schematized in Figure 3. This cavity, built with a spherical mirror M_1 and a plane mirror M_2, contains two quarter-wave plates L_1 and L_2, a circular aperture A, the gain medium subjected to the longitudinal magnetic field B, and an "étalon". The axes of the quarter-wave plates L_1 and L_2 make angles ρ and $\pi/4$ respectively with respect to the x and y axes. The rutile crystal introduces a polarization walk-off between the ordinary and extraordinary paths and the sample cell is located on the ordinary path only.

In order to determine the eigenstates of this cavity, we calculate the 4×4 spatially generalized Jones matrix $M(\nu)$ at frequency ν for one round-trip in the cavity starting in the $+z$ direction

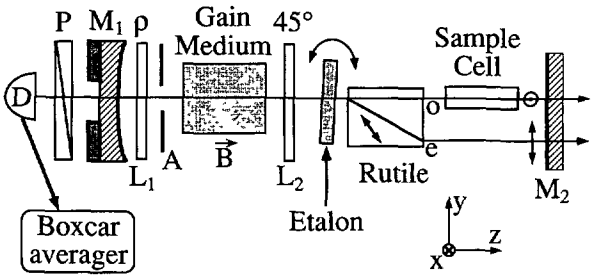

Fig. 3. — Experimental setup.

from mirror M_2:

$$M(\nu) = C^{+}E(\nu)L_2(\pi/4)G(\nu)AL_1(\rho)M_1L_1(\rho)AG(\nu)L_2(\pi/4)E(\nu)C^{-}M_2. \tag{5}$$

These 4×4 matrices are based on a 4-vector description of the light electric fields of the two paths where the two top rows represent the usual Jones vector of the light present on the ordinary path and the two bottom rows represent the usual Jones vector of the light present on the extraordinary path [8]. M_1 and M_2 are the mirrors' matrices which we take as isotropic, leading to:

$$M_1 = r_1 \begin{bmatrix} 1 & 0 & 0 & 0 \\ 0 & 1 & 0 & 0 \\ 0 & 0 & 1 & 0 \\ 0 & 0 & 0 & 1 \end{bmatrix}, \tag{6a}$$

$$M_2 = r_2 \begin{bmatrix} 1 & 0 & 0 & 0 \\ 0 & 1 & 0 & 0 \\ 0 & 0 & 1 & 0 \\ 0 & 0 & 0 & 1 \end{bmatrix}, \tag{6b}$$

where r_1 and r_2 are the amplitude reflection coefficients of the two mirrors. C^{+} and C^{-} are the matrices of the rutile crystal for the $+z$ and $-z$ propagation directions respectively and are given by:

$$C^{+} = \begin{bmatrix} \exp(i\phi_o) & 0 & 0 & 0 \\ 0 & 0 & 0 & 0 \\ 0 & 0 & \exp(i\phi_o) & 0 \\ 0 & \exp(i\phi_e) & 0 & 0 \end{bmatrix}, \tag{7a}$$

$$C^{-} = \begin{bmatrix} \exp(i\phi_o) & 0 & 0 & 0 \\ 0 & 0 & 0 & \exp(i\phi_e) \\ 0 & 0 & \exp(i\phi_o) & 0 \\ 0 & 0 & 0 & 0 \end{bmatrix}, \tag{7b}$$

where ϕ_o and ϕ_e are the dephasings undergone by the ordinary (x) and extraordinary (y) polarizations respectively while propagating through the crystal. $L_1(\rho)$ and $L_2(\pi/4)$ are the Jones matrices of the quarter-wave plates:

$$L_1(\rho) = \begin{bmatrix} l(\rho) & 0 & 0 \\ 0 & 0 & 0 \\ 0 & 0 & l(\rho) \\ 0 & 0 & \end{bmatrix}. \tag{8a}$$

$$L_2(\pi/4) = \frac{1}{\sqrt{2}} \begin{bmatrix} 1 & i & 0 & 0 \\ i & 1 & 0 & 0 \\ 0 & 0 & 1 & i \\ 0 & 0 & i & 1 \end{bmatrix}, \tag{8b}$$

where $l(\rho)$ is the usual 2×2 Jones matrix of the quarter-wave plate with its axes rotated by an angle ρ with respect to the x and y axes:

$$l(\rho) = \begin{bmatrix} \exp\left(i\frac{\pi}{4}\right)\cos^2\rho + \exp\left(-i\frac{\pi}{4}\right)\sin^2\rho & i\sqrt{2}\sin\rho\cos\rho \\ i\sqrt{2}\sin\rho\cos\rho & \exp\left(i\frac{\pi}{4}\right)\sin^2\rho + \exp\left(-i\frac{\pi}{4}\right)\cos^2\rho \end{bmatrix}. \tag{9}$$

A is the matrix of the aperture which selects the ordinary path in the left-hand part of the cavity:

$$A = \begin{bmatrix} 1 & 0 & 0 & 0 \\ 0 & 1 & 0 & 0 \\ 0 & 0 & 0 & 0 \\ 0 & 0 & 0 & 0 \end{bmatrix}. \tag{10}$$

If the "étalon" is only slightly tilted, we can consider it as isotropic and write its matrix in the following way:

$$E(\nu) = e(\nu) \begin{bmatrix} 1 & 0 & 0 & 0 \\ 0 & 1 & 0 & 0 \\ 0 & 0 & 1 & 0 \\ 0 & 0 & 0 & 1 \end{bmatrix}, \tag{11}$$

where $e(\nu)$ is the Airy transmission function of the "étalon". Finally, when the active medium is submitted to the longitudinal magnetic field B, its σ^+ and σ^- gain and dispersion curves are split by the Zeeman effect, leading to the occurrence of a circularly dichroic gain and a small Faraday effect. Neglecting the small Faraday effect, the generalized Jones matrix $G(\nu)$ of the active medium can be written:

$$G(\nu) = \frac{1}{2} \begin{bmatrix} (g_+ + g_-) - i(g_+ - g_-) & 0 & 0 \\ i(g_+ - g_-)(g_+ + g_-) & 0 & 0 \\ 0 & 0 & (g_+ + g_-) - i(g_+ - g_-) \\ 0 & 0 & i(g_+ - g_-)(g_+ + g_-) \end{bmatrix}, \tag{12}$$

where the σ^+ and σ^- gain coefficients g_+ and g_- at frequency ν are given by:

$$g_\pm(\nu) = \exp\left\{ g_0 L \exp\left[-\left(\frac{\nu - \nu_\pm}{ku/(2\pi)} \right)^2 \right] \right\}, \tag{13}$$

where g_0 is the unsaturated gain at line center, ν_+ and ν_- are the center frequencies of the σ^+ and σ^- gain curves ($\nu_+ - \nu_- = 2\Delta\nu_Z$), ku is the Doppler width of the transition and L is the length of the active medium. The development of equation (5) then leads to (neglecting isotropic phase factors):

$$M(\nu) = r_1 r_2 e^2(\nu) g_+(\nu) g_-(\nu) \begin{bmatrix} e^{2i(\phi_c+\rho)} & 0 & 0 & 0 \\ 0 & 0 & 0 & 0 \\ 0 & 0 & 0 & 0 \\ 0 & 0 & 0 & -e^{2i(\phi_c-\rho)} \end{bmatrix}. \tag{14}$$

The resonance condition $M\mathbf{E} = \lambda\mathbf{E}$, where $\mathbf{E}$ is the light electric field and λ the associated eigenvalue, leads to the existence of an ordinary x-polarized eigenstate located on the ordinary

path and an extraordinary y-polarized eigenstate located on the extraordinary path given by:

$$\mathbf{E}_o = \begin{bmatrix} 1 \\ 0 \\ 0 \\ 0 \end{bmatrix}, \tag{15a}$$

$$\mathbf{E}_e = \begin{bmatrix} 0 \\ 0 \\ 0 \\ 1 \end{bmatrix}. \tag{15b}$$

Their eigenvalues are respectively given by:

$$\lambda_o = r_1 r_2 e^2(\nu_o) g_+(\nu_o) g_-(\nu_o) \exp\left[2i(\phi_o + \rho)\right], \tag{16a}$$

$$\lambda_e = -r_1 r_2 e^2(\nu_e) g_+(\nu_e) g_-(\nu_e) \exp\left[2i(\phi_e - \rho)\right], \tag{16b}$$

where the eigenfrequencies of the two eigenstates for a given longitudinal mode labeled by integer p are given by:

$$\nu_o = \frac{c}{2d}\left(p - \frac{\phi_o + \rho}{\pi}\right), \tag{17a}$$

$$\nu_e = \frac{c}{2d}\left(p + \frac{1}{2} - \frac{\phi_e - \rho}{\pi}\right). \tag{17b}$$

Consequently, their frequency difference is given by:

$$v_e - \nu_o = \frac{c}{2d}\left(\frac{1}{2} + \frac{2\rho + \phi_o - \phi_e}{\pi}\right). \tag{18}$$

In the active medium, the electric fields $\mathbf{E}_o^-$ and $\mathbf{E}_e^-$ of these eigenstates propagating in the $-z$ direction can be obtained by propagating the fields $\mathbf{E}_o$ and $\mathbf{E}_e$ through the matrix $L_2 C^-$, leading to:

$$\mathbf{E}_o^- = \frac{1}{\sqrt{2}} \begin{bmatrix} 1 \\ i \\ 0 \\ 0 \end{bmatrix}, \tag{18a}$$

$$\mathbf{E}_e^- = \frac{1}{\sqrt{2}} \begin{bmatrix} i \\ 1 \\ 0 \\ 0 \end{bmatrix}. \tag{18b}$$

Similarly, the electric fields of the eigenstates in the active medium for the $+z$ propagation direction can be obtained by propagating the fields $\mathbf{E}_o$ and $\mathbf{E}_e$ through the matrix $L_1\ L_1\ L_2\ C^-$, leading to:

$$\mathbf{E}_o^+ = \frac{1}{\sqrt{2}} \begin{bmatrix} i \\ 1 \\ 0 \\ 0 \end{bmatrix}, \tag{19a}$$

$$\mathbf{E}_e^+ = \frac{1}{\sqrt{2}} \begin{bmatrix} 1 \\ i \\ 0 \\ 0 \end{bmatrix}. \tag{19b}$$

To summarize these predictions, we can see from the preceding equations that the two eigenstates of a given longitudinal mode are an ordinary and an extraordinary eigenstates which are spatially separated between the rutile crystal and mirror M_2 [equations (15)]. This will permit to introduce the sample gas cell on the path of a single eigenstate, as shown in Figure 3. Their eigenfrequency difference can be tuned to any value by tuning ρ, *i.e.*, by turning quarter-wave plate L_1 [equation (18)]. In particular, the desired frequency difference $c/4d$ between the two eigenstates can be obtained. Moreover, equations (19) show that these ordinary and extraordinary eigenstates are respectively a right-handed and a left-handed helicoidally polarized eigenstates in the active medium [11, 12], *i.e.*, they are made of a σ^+ (respectively σ^-) wave traveling in the $+z$ direction and a σ^- (respectively σ^+) wave propagating in the $-z$ direction, as summarized in Figure 2. This means that these polarization eigenstates fit the eigenvectors of the active medium when submitted to a longitudinal magnetic field, contrary to linearly polarized eigenstates. A peculiarity of these helicoidal eigenstates is that, in the presence of the magnetic field B, they will be amplified in the active medium only for one direction of propagation (see Fig. 2). Moreover, the amplification directions of propagation are opposite for the two orthogonally polarized eigenstates.

The only question which remains to be solved can be seen from Figure 2. This figure exhibits the σ^+ and σ^- gain curves of the active medium. Each of these gain curves can sustain oscillation of the two eigenstates of two different longitudinal modes (two different integers p in the preceding equations). However, we wish to restrain oscillation to the frequencies that coincide with the $^{13}CH_4$ absorption line, *i.e.*, to the eigenstates corresponding to the σ^- gain curve. This is the reason for the introduction of the étalon and of its transmission function $e(\nu)$. Indeed, one can see from the moduli of the eigenvalues of equations (16) that the "étalon" must be designed so that the function $r_1 r_2 e^2(\nu) g_+(\nu) g_-(\nu)$ be much stronger at the σ^- frequencies than at the σ^+ frequencies. For example, the use of a 2 mm-thick silicon plate (refractive index 3.4 at 3.39 μm) is expected to provide a 100% transmission at the σ^+ frequency and a 65% transmission at the σ^- frequency, permitting to turn the undesired eigenstates off (see Fig. 2).

3. Experiment

3.1. Experimental Realization. — The experiment is realized as schematized in Figure 3. The spherical mirror M_1 has a radius of curvature of 2 m and transmits 1.5% of the incident intensity. The plane mirror M_2 transmits 5% of the incident intensity. The length of the cavity is $d = 1.07$ m. The active medium is a 55 cm-long discharge tube with a 3 mm inner diameter and closed with quasi-perpendicular silica windows. It is filled with a 7:1 $^3He - ^{20}Ne$ mixture at a total pressure of 1.1 Torr and is located inside a solenoid which provides the 510 G longitudinal magnetic field. The rutile crystal introduces a 5 mm polarization walk-off, permitting to introduce a 20 cm-long absorption cell on the ordinary axis only. The diameter of the diffracting aperture is 2.2 mm. The "étalon" is made with a 2 mm-thick uncoated silicon plate. It is turned to select only the two eigenstates which are amplified by the σ^- gain curve. A polarizer is introduced in front of the detector D in order to select one of the eigenstates. By tuning the orientation of the quarter-wave plate L_1, one can tune the frequencies of the two oscillating eigenstates so that $\nu_e - \nu_o = c/4d$. By tuning the length of the cavity thanks to a piezoelectric transducer that carries M_1, one then obtains the evolution of the intensity of the extraordinary eigenstate *versus* cavity frequency reproduced in Figure 4a (upper trace). This profile exhibits the two simultaneity regions in which the two eigenstates oscillate and where the measurements will be performed. The zero intensity region in the middle of this profile corresponds to the oscillation of the ordinary eigenstate alone. It is surrounded by the two simultaneity regions in which this ordinary eigenstate oscillates simultaneously

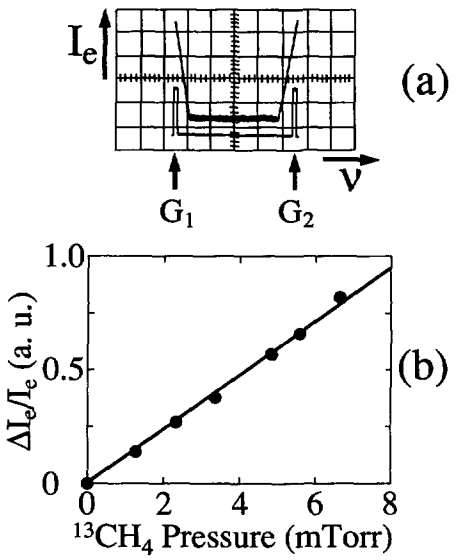

Fig. 4. — a) Evolution of the extraordinary eigenstate intensity *versus* cavity tuning (upper trace). The lower trace displays the symmetrical gates G_1 and G_2 of the boxcar averager which samples the intensity of the extraordinary eigenstate in the vectorial simultaneity region (horizontal axis: 16 MHz per division). b) Evolution of the relative variation of the intensity of the extraordinary eigenstate versus pure $^{13}CH_4$ pressure introduced in the measurement cell.

with the extraordinary eigenstates corresponding to two successive longitudinal modes of the laser. The usefulness of the choice $\nu_e - \nu_o = c/4d$ appears now clearly: it permits to make the profile of Figure 4a symmetrical, allowing us to perform two equivalent measurements in the two simultaneity regions, avoiding any systematic error due to a difference in the losses of two eigenstates. Indeed, the lower trace of Figure 4a represents the two boxcar gates opened to sample the extraordinary intensity in the two simultaneity regions. The sum of these two resulting sampled intensities is then integrated and monitored while the sample gas is introduced inside the cell. During all this procedure, the average cavity length is locked in the symmetrical situation of Figure 4a, so that gates G_1 and G_2 are always opened for the same cavity lengths (for further details upon the experimental detection setup, see Ref. [7]).

With $B = 510$ G, the optical lever effect for $^{13}CH_4$ is experimentally put into evidence by introducing a controlled pressure of pure $^{13}CH_4$ in the sample cell. One then obtains the evolution of the relative variation of the sampled extraordinary eigenstate intensity *versus* $^{13}CH_4$ pressure reproduced in Figure 4b. This figure shows that the obtained signal is linear with the absorber pressure. From the slope of the linear fit of Figure 4b and from the value of the absorption coefficient of $^{13}CH_4$, one can deduce a value of the optical lever factor OL of equation (4) equal to 30. This corresponds in our experimental conditions to a coupling constant C equal to 0.75. Although this value of the optical lever effect is relatively low compared to the values obtained in the case of $^{12}CH_4$, it represents a significant improvement with respect to an extracavity measurement.

3.2. Measurements of Carbon Isotopic Ratios of Methane. — In order to measure the carbon isotopic ratio of a given sample, we make two successive measurements of the concentrations of the two isotopes of carbon in the sample methane. i) With $B = 0$, we obtain

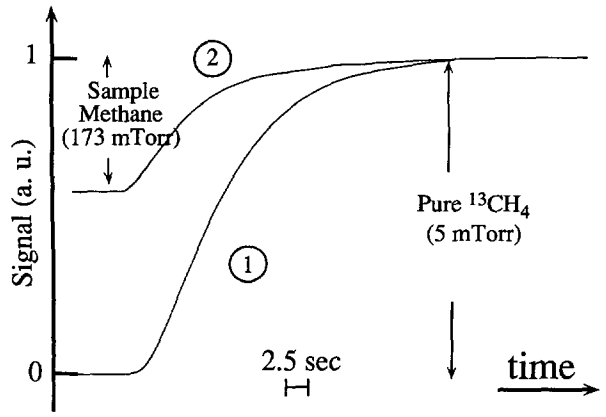

Fig. 5. — Evolution of the relative variation of the intensity of the extraordinary eigenstate *versus* time when 5 mTorr of pure $^{13}CH_4$ are introduced in the cell (Curve 1) and when 173 mTorr of the analyzed methane are introduced in the cell (Curve 2). The time constant of these curves is due to the filling procedure. The real time constant of the experiment is 1 s.

an optical lever factor $OL = 150$ for $^{12}CH_4$. We introduce inside the cell a known quantity of the sample gas, leading to a measurement of the concentration of $^{12}CH_4$. This experiment is similar to the one previously performed for $^{12}CH_4$ with linearly polarized eigenstates [7], except the fact that the laser eigenstates are now helicoidally polarized. ii) With $B = 510$ G, the use of helicoidal eigenstates permits to use the Zeeman effect to probe the $^{13}CH_4$ absorption line with the benefit of the optical lever effect. The system is first calibrated by introducing inside the cell a known pressure of pure $^{13}CH_4$ and recording the corresponding response of the system (*i.e.*, the sampled extraordinary eigenstate intensity, as in Fig. 4a). A known pressure of the unknown methane sample is then introduced inside the empty cell and the corresponding response is also recorded. The results of such recordings for $B = 510$ G are reproduced in Figure 5 for 5 mTorr of pure $^{13}CH_4$ and 173 mTorr of the analyzed methane (natural methane). From these measurements, one obtains the concentration of $^{13}CH_4$ in the unknown sample methane. For the sample of natural methane that we have used here, the ratio of these two measurements leads to a value of the carbon isotopic ratio $^{13}CH_4/^{12}CH_4 = 1.14\% \pm 0.07\%$. The precision of the measurement is given by the standard error observed on six successive measurements of the same sample. In our measurements, the main source of noise is technical noise due to thermal drifts introduced by the solenoid which produces the longitudinal magnetic field and to mechanical vibrations. To test the validity of our measurements, the same sample has also been measured by mass spectroscopy (High resolution mass spectrometer Varian model MAT 311, electron impact, accelerating voltage: 3 kV, 5×10^{-7} mole of methane in the sample), giving a value of $^{13}CH_4/^{12}CH_4 = 1.12\% \pm 0.02\%$.

4. Discussion and Conclusion

In conclusion, we have seen that the generalized Jones matrix formalism permits to design theoretically a laser cavity aimed to measure the carbon isotopic composition of methane. The optical lever effect is obtained in the case of helicoidally polarized eigenstates. These eigenstates are the only ones which permit to reach both carbon isotopes of methane by tuning the magnetic field applied upon the active medium. Moreover, the theoretical predictions are in

agreement with the experiment. This experiment has permitted to measure the $^{13}CH_4/^{12}CH_4$ ratio with an uncertainty of the order of $\pm 0.07\%$, giving results in agreement with our mass spectroscopy measurements. Although the precision of the present experiment is relatively modest, one has to notice the two following points. First, compared to mass spectroscopy, our method is non-destructive. Second, the quantity of methane present in the interaction region in our experiments is of the order of 6×10^{-9} mole (4×10^{15} molecules of methane) for a 20 cm-long optical path. This is a very small quantity compared to the 3×10^{-5} mole of methane (2×10^{19} molecules of methane) which are necessary for high precision mass spectroscopy [13] and compared to the 2×10^{-6} mole of methane (2×10^{18} molecules of methane) probed along a 213 m-long optical path (1.5 m long multipass cell) in reference [6]. Consequently, our method could be particularly efficient to analyze very small quantities of gas, such as the one extracted from the air bubbles present in ice cores and used in glaciology to study the evolution of the climate [1]. Besides, the precision of the present method could certainly be improved by building a monobloc cavity to reduce mechanical vibrations and by reducing the intracavity losses in order to increase the dynamics of the measurement.

Acknowledgments

The authors are happy to thank J. Chappelaz and F. Thibault for their assistance. This work is supported by the Centre National de la Recherche Scientifique, the Direction des Recherches, Etudes et Techniques, and the Conseil Régional de Bretagne.

References

[1] Chappelaz J., Blunier T., Raynaud D., Barnola J.M., Schwander J. and Stauffer B., *Nature* **366** (1993) 443.
[2] Lelieveld J., Crutzen P.J. and Brühl C., *Chemosphere* **26** (1993) 739.
[3] Tyler S.C., *J. Geophys. Research* **91** (1986) 13232.
[4] Quay P.D., King S.L., Stutsman J., Wilbur D.O., Steele L.P., Fung I., Gammon R.H., Brown T.A., Farwell G.W., Grootes P.M. and Schmidt F.H., *Global Biogeochem. Cycles* **5** (1991) 25.
[5] Webster C.R. and May R.D., *Geophys. Research Lett.* **19** (1992) 45.
[6] Schupp M., Bergamaschi P., Harris G.W. and Crutzen P.J., *Chemosphere* **26** (1993) 13; Bergamaschi P., Schupp M. and Harris G.W., *Appl. Opt.* **33** (1994) 7704.
[7] Tran N.H., Jacob D., Le Floch A. and Bretenaker F., *Electron Lett.* **30** (1994) 2026; Jacob D., Tran N.H., Le Floch A. and Bretenaker F., *J. Opt. Soc. Am. B* **12** (1995) 1843.
[8] Bretenaker F. and Le Floch A., *J. Opt. Soc. Am. B* **8** (1991) 230.
[9] Sargent M. III, Scully M.O. and Lamb, W.E. Jr., Laser Physics (Addison-Wesley, Reading, MA, 1974).
[10] Pine A.S., *J. Molec. Spectrosc.* **54** (1975) 132.
[11] Evtuhov V. and Siegman A.E., *Appl. Opt.* **4** (1965) 142.
[12] Kastler A., *C. R. Acad. Sci. B* **271** (1970) 999.
[13] Levin I., Bergamaschi P., Dörr H. and Trapp D., *Chemosphere* **26** (1993) 161.